

University of Groningen

Biointerface topography regulates phenotypic switching and cell apoptosis in vascular smooth muscle cells

Han, Lu; Yin, Qingde; Yang, Liangliang; van Rijn, Patrick; Yang, Yanyan; Liu, Yan; Li, Min; Yan, Mingzhe; Zhou, Qihui; Yu, Tao

Published in:
Biochemical and Biophysical Research Communications

DOI:
[10.1016/j.bbrc.2020.03.038](https://doi.org/10.1016/j.bbrc.2020.03.038)

IMPORTANT NOTE: You are advised to consult the publisher's version (publisher's PDF) if you wish to cite from it. Please check the document version below.

Document Version
Publisher's PDF, also known as Version of record

Publication date:
2020

[Link to publication in University of Groningen/UMCG research database](#)

Citation for published version (APA):

Han, L., Yin, Q., Yang, L., van Rijn, P., Yang, Y., Liu, Y., Li, M., Yan, M., Zhou, Q., Yu, T., & Lian, Z. (2020). Biointerface topography regulates phenotypic switching and cell apoptosis in vascular smooth muscle cells. *Biochemical and Biophysical Research Communications*, 526(3), 841-847. <https://doi.org/10.1016/j.bbrc.2020.03.038>

Copyright

Other than for strictly personal use, it is not permitted to download or to forward/distribute the text or part of it without the consent of the author(s) and/or copyright holder(s), unless the work is under an open content license (like Creative Commons).

The publication may also be distributed here under the terms of Article 25fa of the Dutch Copyright Act, indicated by the "Taverne" license. More information can be found on the University of Groningen website: <https://www.rug.nl/library/open-access/self-archiving-pure/taverne-amendment>.

Take-down policy

If you believe that this document breaches copyright please contact us providing details, and we will remove access to the work immediately and investigate your claim.

Downloaded from the University of Groningen/UMCG research database (Pure): <http://www.rug.nl/research/portal>. For technical reasons the number of authors shown on this cover page is limited to 10 maximum.



Contents lists available at ScienceDirect

Biochemical and Biophysical Research Communications

journal homepage: www.elsevier.com/locate/ybbrc

Biointerface topography regulates phenotypic switching and cell apoptosis in vascular smooth muscle cells

Lu Han ^a, Qingde Yin ^b, Liangliang Yang ^d, Patrick van Rijn ^d, Yanyan Yang ^c, Yan Liu ^c,
Min Li ^c, Mingzhe Yan ^a, Qihui Zhou ^{c,*}, Tao Yu ^{c,*}, Zhexun Lian ^{a,*}

^a Department of Cardiology, The Affiliated Hospital of Qingdao University, Qingdao 266003, China

^b Department of Laboratory Medicine, Linyi Center for Disease Control and Prevention, 276000, China

^c Institute for Translational Medicine, School of Basic Medicine, Qingdao University, Qingdao, 266021, China

^d University of Groningen, W.J. Kolff Institute for Biomedical Engineering and Materials Science, Department of Biomedical Engineering, University Medical Center Groningen, A. Deusinglaan 1, 9713 AV, Groningen, the Netherlands

ARTICLE INFO

Article history:

Received 19 February 2020

Accepted 5 March 2020

Available online xxx

Keywords:

In-stent restenosis

Vascular smooth muscle cells

Phenotypic switching

Apoptosis

Wrinkled topography

Polydimethylsiloxane

ABSTRACT

Background: In-stent restenosis (ISR) is a complex disease that occurs after coronary stenting procedures. The development of quality materials and improvement of our understanding on significant factors regulating ISR are essential for enhancing prognosis. Vascular smooth muscle cells (VSMCs) are the main constituent cells of blood vessel walls, and dysfunction of VMSCs can exacerbate ISR. Accordingly, in this study, we explored the influence of wrinkled material topography on the biological functions of VSMCs. **Methods:** Polydimethylsiloxane with a wrinkled topography was synthesized using elastomer base and crosslinking and observed by atomic force microscopy. VSMC proliferation, apoptosis, and morphology were determined by Cell Counting Kit-8 assays, fluorescence-assisted cell sorting, and phalloidin staining. α -Smooth muscle actin (α -SMA), major histocompatibility complex (MHC), and calponin 1 (CNN-1) expression levels were measured by quantitative real-time polymerase chain reaction and western blotting. Moreover, p53 and cleaved caspase-3 expression levels were evaluated by western blotting in VSMCs to assess apoptotic induction.

Results: Surface topographies were not associated with a clear orientation or elongation of VSMCs. The number of cells was increased on wrinkled surfaces (0.7 μ m in amplitude, and 3 μ m in wavelength [W3]) compared with that on other surfaces, contributing to continuously increased cell proliferation. Moreover, interactions of VSMCs with the W3 surface suppressed phenotypic switching, resulting in ISR via regulation of α -SMA, calponin-1, and SM-MHC expression. The surface with an amplitude of 0.05 μ m and a wavelength of 0.5 μ m (W0.5) promoted apoptosis by inducing caspase 3 and p53 activities.

Conclusion: Introduction of aligned topographies on biomaterial scaffolds could provide physical cues to modulate VSMC responses for engineering vascular constructs. Materials with wrinkled topographies could have applications in the development of stents to reduce ISR.

© 2020 Elsevier Inc. All rights reserved.

1. Introduction

In-stent restenosis (ISR), a fibroproliferative process of the vessel wall structure in response to injury, results in neointima formation and is the main disadvantage of percutaneous coronary procedures caused by abnormal accumulation of VSMCs and

defects in the extracellular matrix environment [1,2]. The overall rate of restenosis with treatment based on existing commercial products and scientific studies is approximately 20–37% [3–5]. Although some methods, such as scaffold design and the use of drug-eluting stents, have greatly improved therapeutic effects, ISR remains a major clinical problem which can affect the adverse effects of drugs, resulting in damage to the vascular structure and disruption of heart function [6]. Because the molecular mechanisms of this process remain largely unknown, dysfunction of VSMCs, which stimulate inflammation, phenotypic switching, and fibrotic reactions, is thought to play an important role [7].

* Corresponding authors.

E-mail addresses: lyang@umcg.nl (L. Yang), p.van.rijn@umcg.nl (P. van Rijn), qihuizhou@qdu.edu.cn (Q. Zhou), yutao0112@qdu.edu.cn (T. Yu), lianzx566@163.com (Z. Lian).

<https://doi.org/10.1016/j.bbrc.2020.03.038>

0006-291X/© 2020 Elsevier Inc. All rights reserved.

VSMCs are the major cell type found in human blood vessel walls and function to maintain constant vascular tone, stabilize normal blood pressure, and regulate blood flow distribution. In particular, VSMCs exhibit significant apparent plasticity, allowing them to adapt quickly to changes in the surrounding environment; this feature can play important roles in vascular diseases, such as restenosis and atherosclerosis after percutaneous coronary angioplasty [8]. Mature VSMCs have two main cellular patterns of protein expression, viz., contractile and synthetic phenotypes. VSMCs of the contractile phenotype are highly expressed in adult blood vessels and predominantly secrete contractile proteins, such as α -SMA, MHC, and CNN-1 [9]. However, VSMCs of the synthetic phenotype in the pathological state not only have decreased ability to express these proteins but also show enhanced proliferation, migration, and protease synthesis related to extracellular matrix components [10]. Following exogenous stimulation by cytokines, oxygen radicals, and liposomes, VSMCs will actively regulate their own expression phenotypes, significantly reducing the expression of differentiation markers, improving the ability to proliferate, enhancing migration capacity, and synthesizing extracellular matrix components to participate in the formation of the intima; abnormal hyperplasia of the vascular intima may be a root cause of many cardiovascular diseases [11]. According to previous studies, phenotypic switching of VSMCs is an important signal of restenotic remodeling in ISR [12]. VSMCs treated by percutaneous coronary procedures acquire myofibroblastic-like cell properties with the loss of desmin expression and increased production of extracellular matrix components [13]. Thus, it is important to determine the mechanisms regulating cell phenotypic switching of VSMCs during treatment.

The influence of material physical factors, such as hardness, rigidity, shear force, surface structure, and spatial composition, on regulating cell phenotypic switching and apoptosis has attracted much attention. For example, Smally et al. found that tumors cultured in three-dimensional (3D) conditions showed significant differences in RNA fragmentation, suggesting changes in behavior and proliferation of cells [14]. Additionally, Murat et al. investigated the interactions between the human mesenchymal stem cells (hMSCs) and hydrogels with lamellar or hexagonal surface wrinkles and showed that hMSCs exhibited high aspect ratios on these hydrogels, accelerating the speed of differentiation into an osteogenic lineage [15]. Thus, we assumed that biomaterials with certain physical factors could effectively modulate the phenotypic switching of VSMCs to reduce the incidence of abnormal cell proliferation and apoptosis in ISR.

The biomaterial polydimethylsiloxane (PDMS) is a relatively inexpensive, US Food and Drug Administration-approved material that is easy to process and has commonly been used in transplant medicine and as a tissue engineering scaffold [16]. Zhou et al. showed that the nano directional gradient structure fabricated by PDMS was able to guide directional cell contacts as a high-throughput screening platform [17]. However, the effects of PDMS on VSMC behaviors have not yet been reported.

Accordingly, in this study, we investigated the effects of the wrinkled topography formed by PDMS on the behaviors of VSMCs. Our results are expected to provide important insights into the regulatory effects of materials with wrinkled topographies on VSMCs and ISR.

2. Materials and methods

2.1. Synthesis and characterization of PDMS scaffolds

PDMS scaffolds were synthesized as described previously [17–19]. Briefly, PDMS was synthesized as a mixture containing the elastomer base and a crosslinker at a weight ratio of 10:1. The

mixture was vigorously stirred with a spatula, placed in vacuum dryer for degassing until bubbles disappeared completely, and then deposited onto a Petri dish. The material was cured at 70 °C overnight. To form the wrinkled structure, the prepared PDMS substrate was uniaxially stretched to a strain of 10–30% of the original length using a specific stretching machine and oxidized by air plasma at different pressures and for various times. Next, the wrinkled topographies were fabricated when the strain was released (Table 1). The wrinkled topography of PDMS was determined by atomic force microscopy (AFM; Nanoscope V Dimension 3100 microscope; Veeco, USA).

2.2. Cell culture and seeding

VSMCs were purchased from the Type Culture Collection of China (Chinese Academy of Sciences, Shanghai, China) and cultured in a 37 °C 5% CO₂ humidified incubator. The medium consisted of Dulbecco's modified Eagle's medium (Gibco, Grand Island, NY, USA) containing 1% penicillin-streptomycin (Solarbio Science & Technology Co., Beijing, China) and 10% fetal bovine serum.

2.3. Cell proliferation and apoptosis

We evaluated the proliferation of VSMCs using a Cell Counting Kit-8 (CCK-8; 7Sea-Cell Counting Kit, Shanghai). VSMCs were seeded at 2×10^4 cells/well onto substrates in 24-well plates and incubated for 1 or 3 days. CCK-8 solution was then added to each well, and samples were evaluated according to the manufacturer's instructions. Plates were incubated for 1 h at 37 °C, and absorbance was measured using a microplate reader (BioTek, Synergy H1/H1M; USA) at a wavelength of 450 nm.

Annexin V-fluorescein isothiocyanate (FITC)/propidium iodide (PI; Yeasen, USA) staining was used to detect apoptosis in VSMCs. Briefly, VSMCs were grown on 24-well plates containing the above-described substrates for 3 days, washed once with PBS, and then stained with PI and Annexin V-FITC solution in PBS. We then randomly selected five regions from each well for cell counting and calculated the percentage of apoptotic VSMCs among the total number of cells.

2.4. Cell morphology assay

VSMCs were seeded at 2×10^4 cells/well onto substrates in 24-well plates and cultured for 24 h. After aspiration of the old medium, cells were fixed with ice-cold 4% paraformaldehyde (Solarbio) for 10 min. Cells were then permeabilized with 0.5% Triton X-100 (Solarbio), stained with FITC phalloidin (Solarbio) and 4',6-diamidino-2-phenylindole (DAPI; Solarbio), and observed with a fluorescence microscope (Nikon A1 MP; Japan).

2.5. Measurement of gene expression

For measurement of gene expression, we seeded VSMCs onto substrates in 24-well plates at a density of 2×10^4 cells/well and cultured the cells for 3 days. The mRNA levels of α -SMA, CNN-1, osteopontin (OPN), and MHC were then evaluated by qRT-PCR. Briefly, total RNA was extracted from cells using TRIzol (Invitrogen, Grand Island, NY, USA). cDNA was then reverse transcribed using a FastKing RT Kit (Vazyme Biotech, Nanjing, China). Finally, qRT-PCR was performed using a Super Real PreMix Plus (SYBR Green) kit (Yeasen Biotech Co., Ltd., Shanghai, China) and an ABI Prism 7500 sequence detection system (Applied Biosystems, Foster City, CA, USA). Before processing the data, all PCR results were normalized to the expression levels of the glyceraldehyde 3-phosphate dehydrogenase (GAPDH) gene. Data were analyzed

Table 1
Synthesis conditions for PDMS scaffolds with different dimensions.

PDMS substrate	Ratio of prepolymer and crosslinker	Plasma pressure (Pa)	Oxidation time (s)	Stretched percent (%)
Flat	10:1	–	–	0
W0.5A0.05	10:1	1862	60	30
W3A0.7	10:1	3.325	20	30
W10A3.5	10:1	3.325	650	20

W and A are abbreviations for wavelength and amplitude, respectively. The units of W and A were μm .

using the $2^{-\Delta\text{Ct}}$ method. All primer sequences used for qRT-PCR are listed in Table 2.

2.6. Western blotting analysis

VSMCs were seeded at 2×10^4 cells/well onto substrates in 24-well plates and cultured for 3 days. The VSMC cultures were washed with PBS, and 50 μL of a buffer containing RIPA lysis buffer supplemented with 1% phenylmethylsulfonyl fluoride and 0.1% protease inhibitor mixture (Beijing Solarbio Science & Technology Co., Beijing, China) was added to each well. Cells were incubated at 4 °C for 20 min and then collected in 1.5-mL centrifuge tubes. Next, the centrifuge tubes were centrifuged at 12000 \times g for 15 min at 4 °C. A BCA analysis kit (Beijing Solarbio Science & Technology Co.) was used to measure protein concentrations. Proteins were then separated by sodium dodecyl sulfate polyacrylamide gel electrophoresis on 12% gels (EpiZyme, Shanghai, China) and transferred to polyvinylidene fluoride membranes (Merck Millipore, USA). After blocking the membranes with 5% skim milk for 1 h at room temperature, the membranes were incubated with primary antibodies which were all purchased from Cell Signaling Technology (Danvers, MA, USA) at 4 °C overnight. Membranes were then washed three times with Tris-HCl-buffered saline with Tween 20 and incubated with corresponding secondary antibodies with horseradish peroxidase. After washing again three times, protein bands on the membranes were visualized with a Fusion FX7 Multifunction imaging system (Vilber, France) and analyzed with Image J (Java 1.8.0–172).

2.7. Statistical analysis

All data presented in this paper are presented as means \pm standard deviations of at least three independent experiments or an experiment performed with three samples for *in vitro* experiments. Statistical analysis was carried out using GraphPad Prism 7 software, and Tukey's multiple comparison tests were used to make nonparametric comparisons between groups.

3. Results and discussion

3.1. Synthesis and characterization of PDMS scaffolds

Synthesis of PDMS scaffolds was demonstrated in our previous study, and the relevant conditions and results are summarized in Table 1 [17,18]. The degree of variation in wrinkled topography was

Table 2
Primer sequences for genes evaluated in this study.

Gene	Forward primer sequence (5'–3')	Reverse primer sequence (3'–5')
GAPDH	TATTC1CTGATTGGTCGTA	ATGGCAACAATATCCACT
α -SMA	CTATGAGGGCTATGCCTTGCC	GCTCAGCAGTAGTAACGAAGGA
CNN-1	CTGTCAGCCGAGGTTAAGAAC	GAGGCCGTCATGAAGTTGTT
MHC	CGCCAAGAGACTCGTCTGG	TCITTCACCAACCGTGACCTTC
OPN	GAAGTTTCGACACCTGACAT	GTATGCACCATTCAACTCCTCG

determined by AFM. By changing the plasma pressure and oxidation time, the PDMS substitutions showed wavelengths of 0.5–10 μm and amplitudes of 0.05–3.5 μm at a constant crosslinker to prepolymer ratio of 10:1. We named the four experimental groups according to their wavelengths (flat, W0.5, W3, and W10). Notably, the percentage of unidirectional strain was inversely related to plasma pressure and oxidation time, meeting the relevant parameters for application as a high-throughput screening platform to evaluate the impact on cell behavior [20]. Previous studies have suggested that the ideal material should have a wavelength of 0.45–0.75 μm and an amplitude of 0.08–0.18 μm for appropriate cell behaviors [17]. Thus, the PDMS fabricated in this study was within the appropriate range for an ideal material with which to measure the effects on VSMCs.

3.2. Effects of the wrinkled topography on VSMC viability

Cell viability on a substrate is greatly influenced by the properties of the biological interface with the substrate [21]. To demonstrate the capacity of PDMS to support cell attachment and subsequent cellular array formation, VSMCs were incubated on materials with different topographies in 24-well culture plates for 1 or 3 days, and CCK-8 assays were used to quantify cell numbers in each well. VSMC number, density, elongation, and orientation on wrinkled material surfaces were evaluated using AFM (Fig. 1A). On day 1, W3 had a significantly higher cell number and density ($P < 0.001$) than the other three groups (Fig. 1B and C, 2A), suggesting that the modified materials could support the proliferation of VSMCs.

Detection of cell morphology can also partially reflect cell viability. Thus, we next evaluated the morphology of VSMCs on different wavelengths of PDMS using fluorescence microscopy. No differences in cell elongation or orientation were observed (Fig. 1D and E). The highly aligned topology appeared to support cell viability and growth, and similar results were obtained for individual cells and confluent cellular islands. Moreover, compared with the flat group, a slight difference in cell morphology was also observed on the W0.5 and W10 surfaces (Fig. 1A). Thus, we concluded that VSMCs cultured on PDMS with a wrinkled topography was enhanced.

3.3. Wrinkled topography regulated phenotypic transformation in VSMCs

As reported previously, deregulation of VSMC phenotypic transformation plays an essential role in vascular remodeling in some vascular diseases, such as hypertension and atherosclerosis [22,23]. Because cell numbers increased after W3 treatment, we next evaluated the effects of increased proliferation on phenotypic switching. First, we explored the contractile phenotypic properties of treated VSMCs. Wrinkle topographies are related to modulation of the VSMC phenotype towards a contractile state, with significantly increased expression of early (α -SMA), mid (CNN-1), and late stage (SM-MHC) contractile proteins [24,25]. In this study, we also detected significantly higher α -SMA, CNN-1, and SM-MHC mRNA

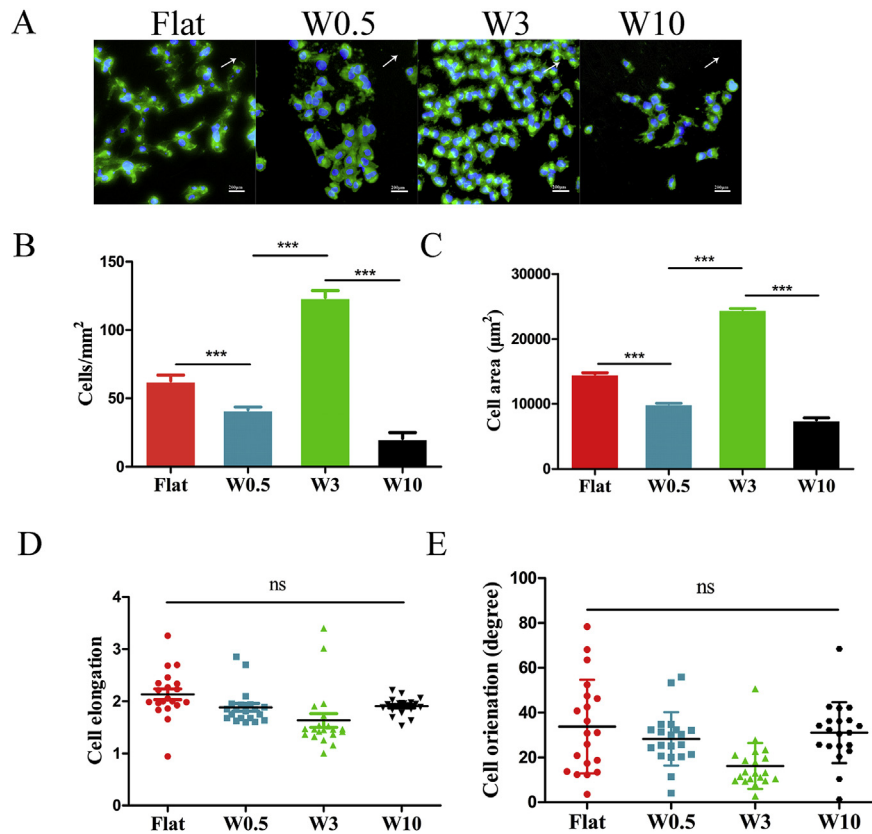


Fig. 1. PDMS wrinkle formation and characterization in VSMCs. **A:** Morphology of the VSMCs grown on different wavelengths of PDMS, as analyzed using a fluorescence microscope after culture for 24 h. Green: phalloidin in cell fibers; blue: DAPI in cell nuclei. **B:** Cell density. **C:** Spreading area. **D:** Elongation. **E:** Orientation. Data are reported as means \pm standard deviations by random sampling monitoring from images ($n = 20$ cells). White arrows: direction of the wrinkles. *** $p < 0.001$. ns: not significant. (For interpretation of the references to colour in this figure legend, the reader is referred to the Web version of this article.)

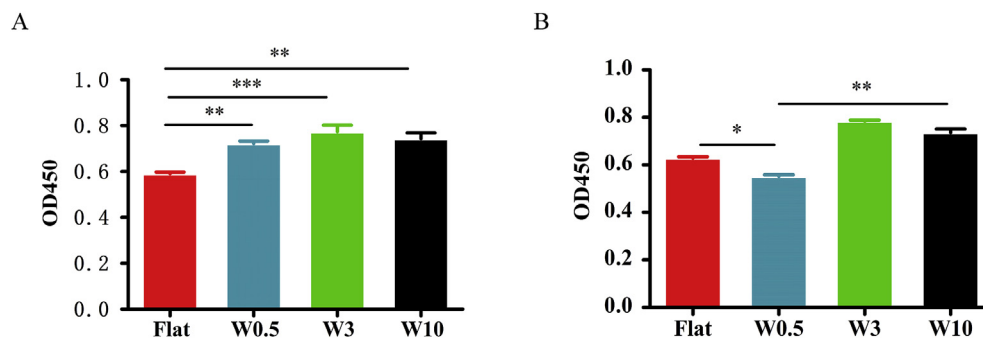


Fig. 2. Effects of the wrinkled topography on the viability of VSMCs. Cell viability was analyzed using CCK-8 assays. VSMCs were cultured on the wrinkled PDMS substrates with different topography dimensions for **A:** 1 day or **B:** 3 days. * $p < 0.05$, ** $p < 0.01$, *** $p < 0.001$.

levels in VSMCs cultured on W3 ($P < 0.05$) compared with that on the other types of materials (Fig. 3A–C). Similar results were obtained in an analysis of protein expression levels by western blotting (Fig. 3E). Additionally, the expression levels of these contractile-related proteins increased in a concentration-dependent manner, with significant differences observed for the W3 group ($P < 0.05$) compared with that in other groups (Fig. 3E–H). These findings indicated that W3-treated VSMCs exhibited anti-atherosclerosis activity, suggesting potential applications of the W3 material in stent design in the future.

Inflammatory markers are often developed as potential therapeutic factors in cardiovascular diseases related to metabolic

dysregulation of Ca^{2+} , nitric oxide, and reactive oxygen species as well as oxidative stress factors and gene deletions [26–28]. Although no genes have been identified as specific markers of inflammation in VSMCs, the phenotypic functions of VSMCs can be determined by evaluating the expression of a combination of contractile characteristic proteins and proteins related to the synthetic phenotype. For example, OPN was previously identified as an important synthetic protein marker [29]. In our study, there were no differences in the expression of OPN among the groups (Fig. 3D).

Taken together, these findings suggested that W3 material promoted the cell contractile phenotype, which could regulate phenotypic transformation in VSMCs.

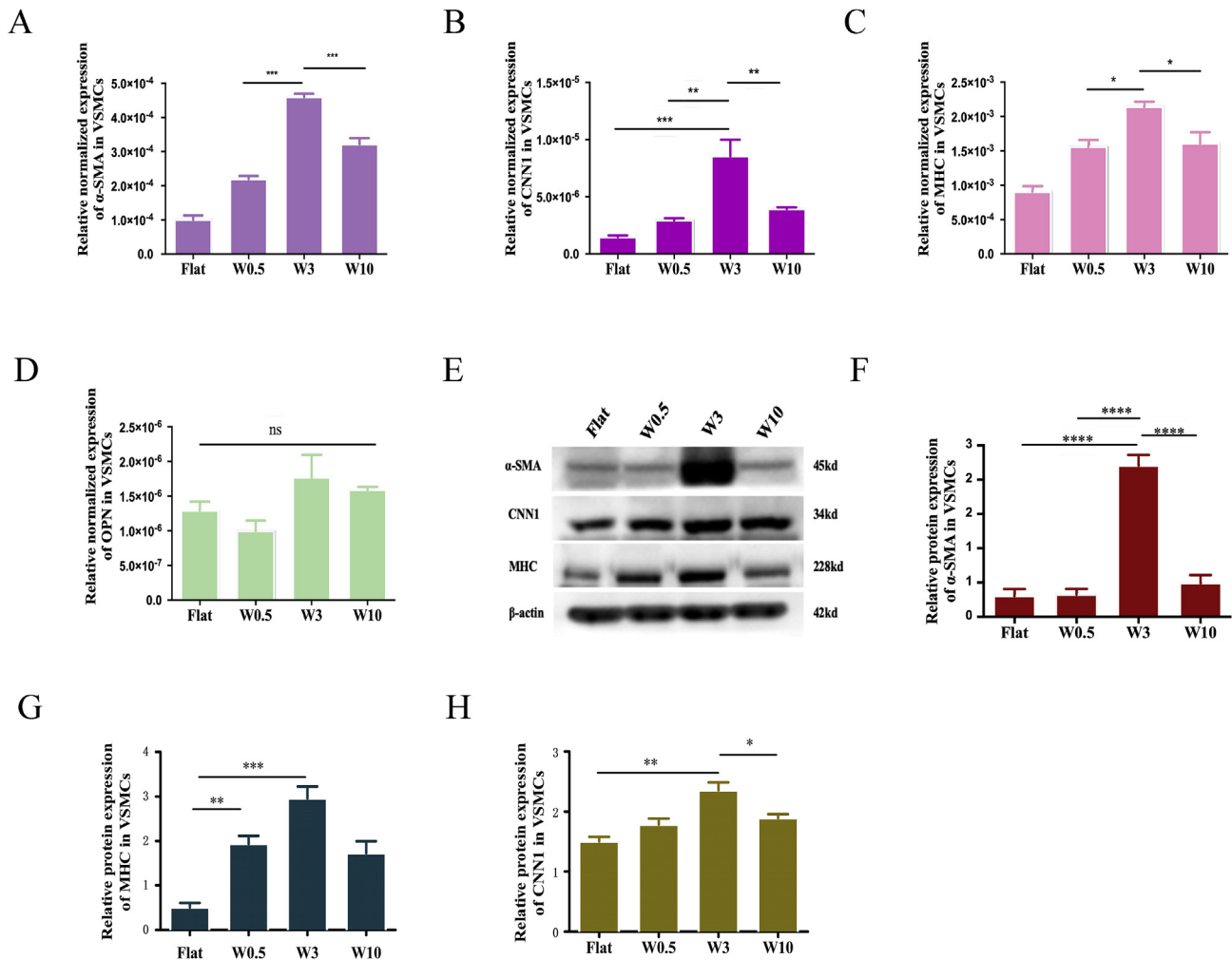


Fig. 3. Effects of the wrinkled topographies on phenotypic transformation in VSMCs. Quantitative real-time polymerase chain reaction was used to evaluate relative mRNA expression levels of **A:** α -SMA, **B:** *CNN-1*, **C:** *MHC*, and **D:** *OPN* genes. **E:** Western blot analysis of **F:** α -SMA, **G:** *MHC*, and **H:** *CNN-1* proteins expression from cells grown on wrinkled topographies for 3 days. * $p < 0.05$, ** $p < 0.01$, *** $p < 0.001$, **** $p < 0.0001$. ns: not significant.

3.4. Effects of the wrinkled topography on apoptosis via activating of caspase 3 and p53 in VSMCs

In addition to cell proliferation, VSMC numbers are also closely related to apoptosis. Thus, we next evaluated apoptosis in VSMCs after culture on wrinkled surfaces for 3 days. Analysis of the apoptotic percentages (Fig. 4) demonstrated that cell survival was lowest in the W0.5 group (early apoptosis: 4.8%; late apoptosis: 18.8%; Fig. 4A). On day 3, the lowest cell numbers were also detected in this group (Fig. 2B), further supporting the induction of apoptosis by the W0.5 material. For VSMCs treated with the other three types of materials, the results of apoptosis assays and western blotting were also consistent with CCK-8 assays on day 3 of cell culture.

VSMCs making up vessel walls can both induce and activate apoptosis. However, apoptosis and mitosis are not easily triggered in normal adult arteries [30]. Some local disease-related factors, such as inflammatory cytokines, modified cholesterol, and abnormal blood pressure and flow, may upset the balance of proliferation and apoptosis, and when apoptosis predominates, disease may develop. Thus, because of the involvement of apoptosis of VSMCs in arteriosclerosis, W0.5 may be used to model atherosclerosis in future scientific studies.

Moreover, according to previous reports, p53 and cleaved caspase-3 are key proteins that regulate apoptosis in VSMCs. Thus, in order to further explore the mechanisms through which the materials with wrinkled topographies caused apoptosis, we performed Western blot analysis of p53 and cleaved caspase-3. As shown in Fig. 4, there was a dramatic increase in the expression levels of these well-known apoptotic markers in VSMCs grown with W0.5 compared with that in the other groups (Fig. 4D–F). Overall, these findings suggested that PDMS with a wrinkled topography could have a negative influence on VSMC behaviors.

4. Conclusions

Owing to the popularity of percutaneous coronary intervention, the incidence of ISR related to bare-metal stents (BMSs) has increased. To overcome this limitation, research have developed drug-eluting stents (DESs). However, although DESs significantly reduce the incidence of ISR, ISR still occurs in 5–10% of patients [31]. ISR is commonly caused by BMS rupture, incomplete expansion, poor adherence, inappropriate stent size, drug resistance, or lack of endothelial coverage by the stent. Mechanistically, endothelial injury or dysfunction, neointimal proliferation, inflammation, and phenotypic transformation of VSMCs are

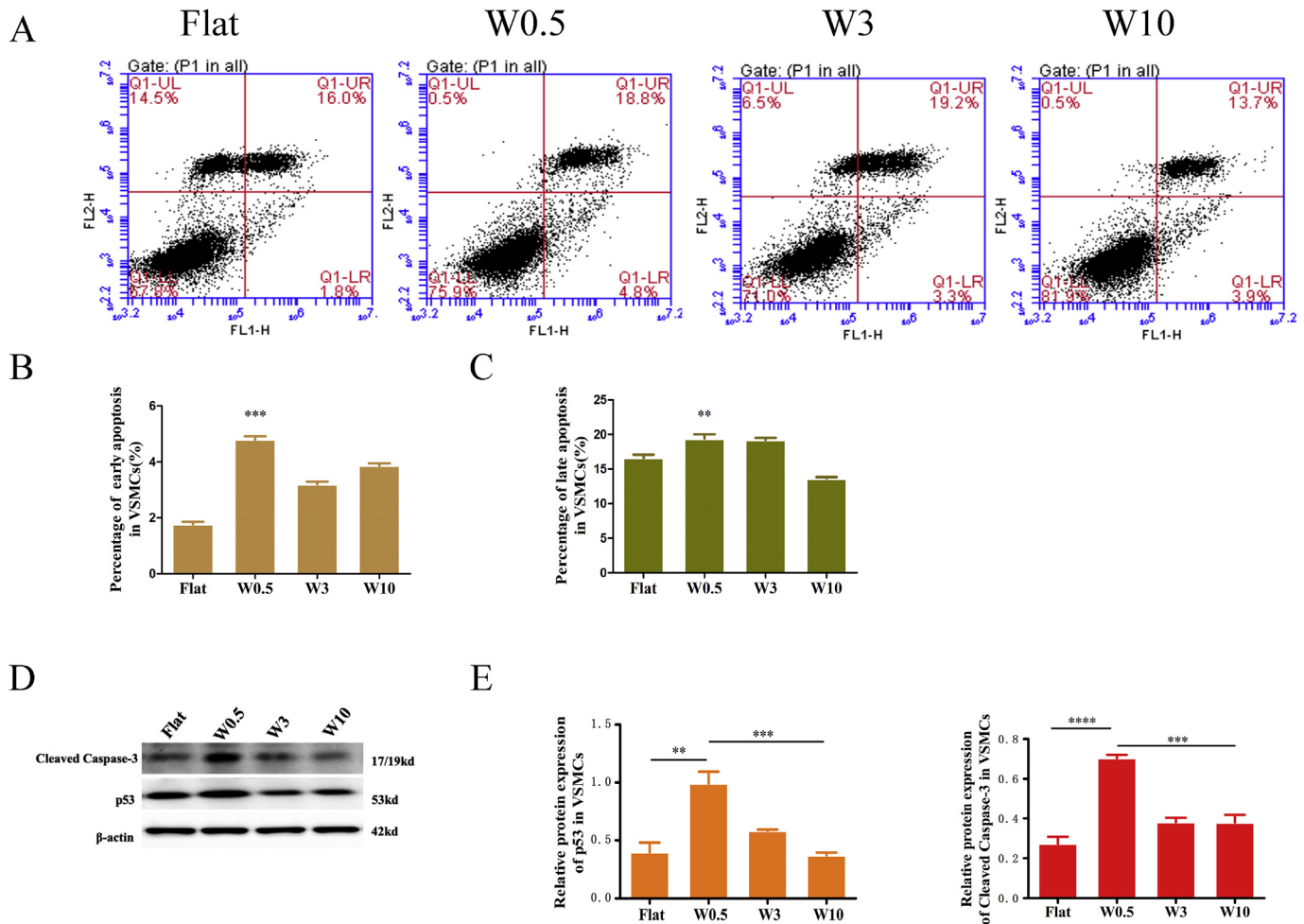


Fig. 4. Effects of the wrinkled topography on apoptosis in VSMCs. **A:** Flow cytometry images of VSMCs after culture on the different types of PDMS for 1 day. **B:** Percentage of VSMCs in early stage apoptosis. **C:** Percentage of VSMCs in late stage apoptosis. **D:** Western blot analysis of p53 and cleaved caspase-3 protein expression in cells cultured on the wrinkled topographies for 3 days. **(E, F):** The quantization of bands in Western blot by Image J software. ** $p < 0.01$, *** $p < 0.001$, **** $p < 0.0001$.

common features of ISR. Stent materials are important factors affecting the occurrence of ISR. Accordingly, in this study, we evaluated the effects of the topography of biointerfaces on ISR in order to improve our understanding of the regulatory mechanisms and factors involved in ISR.

Our results showed that PDMS with a wrinkled topography significantly affected the phenotypic transition and apoptosis of VSMCs. In particular, the W3A0.7 type material had anti-atherosclerotic effects and suppressed the phenotypic transformation of VSMCs. Therefore, introduction of aligned topographies on biomaterial scaffolds could provide physical cues to modulate VSMC responses for engineering vascular constructs. Importantly, PDMS is inexpensive and can greatly reduce the cost of stent materials. Our results also showed that the W0.5A0.05 material promoted the apoptosis of VSMCs through a mechanism involving p53 and caspase-3. Thus, this material could have applications as a model of *in vitro* atherosclerosis. Further studies in animal models are also required to confirm our findings.

However, there also remains several limitations in our study. Firstly, the detailed mechanism of the regulatory effects of materials with wrinkled topographies on VSMCs needs further research. Secondly, how about the effects of other vascular cells while interplaying with wrinkled topographies? Whether they will show the similar regulatory roles? Thirdly, there was no relevant animal experiments were performed, we are not clear whether the

regulatory effect would be observed or not *in vivo*. All these challenges needs more deep research in future.

In conclusion, our findings provided insights into the regulatory effects of materials with wrinkled topographies on VSMCs and could facilitate the development of vascular stents. Furthermore, as a potential new biomaterial, PDMS-based materials with a wrinkled topography could be also used in studies of cell therapy, drug development, and 3D printing for implantation in humans.

Declaration of competing interest

The authors declare no conflict of interests.

Acknowledgements

The authors are very grateful for financial support from the National Natural Science Foundation of China (grant no. 81870331, 31900957, 31701208), Shandong Provincial Natural Science Foundation (grant no. ZR2019QC007), Innovation and Technology Program for the Excellent Youth Scholars of Higher Education of Shandong province (grant no. 2019KJE015), China Postdoctoral Science Foundation (grant no. 2019M652326), and Scientific Research Foundation of Qingdao University (grant no. DC190009689).

References

- [1] C. Indolfi, A. Mongiardo, A. Curcio, D. Torella, Molecular mechanisms of in-stent restenosis and approach to therapy with eluting stents, *Trends Cardiovasc. Med.* (2003), [https://doi.org/10.1016/S1050-1738\(03\)00038-0](https://doi.org/10.1016/S1050-1738(03)00038-0).
- [2] N.A. Scott, Restenosis following implantation of bare metal coronary stents: pathophysiology and pathways involved in the vascular response to injury, *Adv. Drug Deliv. Rev.* (2006), <https://doi.org/10.1016/j.addr.2006.01.015>.
- [3] M.S. Lee, G. Banka, In-stent restenosis, *Interv. Cardiol. Clin.* (2016), <https://doi.org/10.1016/j.iccl.2015.12.006>.
- [4] A.K. Mitra, D.K. Agrawal, In stent restenosis: bane of the stent era, *J. Clin. Pathol.* (2006), <https://doi.org/10.1136/jcp.2005.025742>.
- [5] A. Kastrati, A. Schömig, S. Elezi, H. Schühlen, J. Dirschinger, M. Hadamitzky, A. Wehinger, J. Hausleiter, H. Walter, F.J. Neumann, Predictive factors of restenosis after coronary stent placement, *J. Am. Coll. Cardiol.* (1997), [https://doi.org/10.1016/S0735-1097\(97\)00334-3](https://doi.org/10.1016/S0735-1097(97)00334-3).
- [6] M. Santin, P. Colombo, G. Bruschi, Interfacial biology of in-stent restenosis, *Expet Rev. Med. Dev.* (2005), <https://doi.org/10.1586/17434440.2.4.429>.
- [7] R. Köster, D. Vieluf, M. Kiehn, M. Sommerauer, J. Kahler, S. Baldus, T. Meinertz, C.W. Hamm, Nickel and molybdenum contact allergies in patients with coronary in-stent restenosis, *Lancet* (2000), [https://doi.org/10.1016/S0140-6736\(00\)03262-1](https://doi.org/10.1016/S0140-6736(00)03262-1).
- [8] M.R. Alexander, G.K. Owens, Epigenetic control of smooth muscle cell differentiation and phenotypic switching in vascular development and disease, *Annu. Rev. Physiol.* (2012), <https://doi.org/10.1146/annurev-physiol-012110-142315>.
- [9] M.R. Bennett, S. Sinha, G.K. Owens, Vascular smooth muscle cells in atherosclerosis, *Circ. Res.* (2016), <https://doi.org/10.1161/CIRCRESAHA.115.306361>.
- [10] H.J. Sung, S.G. Eskin, Y. Sakurai, A. Yee, N. Kataoka, L.V. McIntire, Oxidative stress produced with cell migration increases synthetic phenotype of vascular smooth muscle cells, *Ann. Biomed. Eng.* (2005), <https://doi.org/10.1007/s10439-005-7545-2>.
- [11] S.A. Steitz, M.Y. Speer, G. Curinga, H.Y. Yang, P. Haynes, R. Aebersold, T. Schinke, G. Karsenty, C.M. Giachelli, Smooth muscle cell phenotypic transition associated with calcification: upregulation of Cbfa1 and downregulation of smooth muscle lineage markers, *Circ. Res.* (2001), <https://doi.org/10.1161/hh2401.101070>.
- [12] D. Skowasch, A. Jabs, R. Andrié, S. Dinkelbach, B. Lüderitz, G. Bauriedel, Presence of bone-marrow- and neural-crest-derived cells in intimal hyperplasia at the time of clinical in-stent restenosis, *Cardiovasc. Res.* (2003), <https://doi.org/10.1016/j.cardiores.2003.09.001>.
- [13] G.K. Owens, Regulation of differentiation of vascular smooth muscle cells, *Physiol. Rev.* (1995), <https://doi.org/10.1152/physrev.1995.75.3.487>.
- [14] K.S.M. Smalley, M. Lioni, M. Herlyn, Life isn't flat: taking cancer biology to the next dimension, *In Vitro Cell. Dev. Biol. Anim.* (2006), <https://doi.org/10.1290/0604027.1>.
- [15] M.P. Lutolf, P.M. Gilbert, H.M. Blau, Designing materials to direct stem-cell fate, *Nature* (2009), <https://doi.org/10.1038/nature08602>.
- [16] A.J.T. Teo, A. Mishra, I. Park, Y.J. Kim, W.T. Park, Y.J. Yoon, Polymeric biomaterials for medical implants and devices, *ACS Biomater. Sci. Eng.* (2016), <https://doi.org/10.1021/acsbomaterials.5b00429>.
- [17] Q. Zhou, P.T. Kühn, T. Huisman, E. Nieboer, C. Van Zwol, T.G. Van Kooten, P. Van Rijn, Directional nanotopographic gradients: a high-throughput screening platform for cell contact guidance, *Sci. Rep.* (2015), <https://doi.org/10.1038/srep16240>.
- [18] Q. Zhou, P. Wünnemann, P.T. Kühn, J. de Vries, M. Helmin, A. Böker, T.G. van Kooten, P. van Rijn, Mechanical properties of aligned nanotopologies for directing cellular behavior, *Adv. Mater. Interfaces* (2016), <https://doi.org/10.1002/admi.201600275>.
- [19] Q. Zhou, O. Castañeda Ocampo, C.F. Guimarães, P.T. Kühn, T.G. Van Kooten, P. Van Rijn, Screening platform for cell contact guidance based on inorganic biomaterial micro/nanotopographical gradients, *ACS Appl. Mater. Interfaces* 9 (2017) 31433–31445, <https://doi.org/10.1021/acsami.7b08237>.
- [20] M.P. Wolf, G.B. Salieb-Beugelaar, P. Hunziker, PDMS with designer functionalities—properties, modifications strategies, and applications, *Prog. Polym. Sci.* (2018), <https://doi.org/10.1016/j.progpolymsci.2018.06.001>.
- [21] X.Q. Brown, K. Ookawa, J.Y. Wong, Evaluation of polydimethylsiloxane scaffolds with physiologically-relevant elastic moduli: interplay of substrate mechanics and surface chemistry effects on vascular smooth muscle cell response, *Biomaterials* (2005), <https://doi.org/10.1016/j.biomaterials.2004.08.009>.
- [22] H.N. Siti, Y. Kamisah, J. Kamsiah, The role of oxidative stress, antioxidants and vascular inflammation in cardiovascular disease (a review), *Vasc. Pharmacol.* (2015), <https://doi.org/10.1016/j.vph.2015.03.005>.
- [23] A. Caillon, E.L. Schiffrin, Role of inflammation and immunity in hypertension: recent epidemiological, laboratory, and clinical evidence, *Curr. Hypertens. Rep.* (2016), <https://doi.org/10.1007/s11906-016-0628-7>.
- [24] R. Bandopadhyay, C. Orte, J.G. Lawrenson, A.R. Reid, S. De Silva, G. Allt, Contractile proteins in pericytes at the blood-brain and blood-retinal barriers, *J. Neurocytol.* (2001), <https://doi.org/10.1023/A:1011965307612>.
- [25] B. Hinz, D. Mastrangelo, C.E. Iselin, C. Chaponnier, G. Gabbiani, Mechanical tension controls granulation tissue contractile activity and myofibroblast differentiation, *Am. J. Pathol.* (2001), [https://doi.org/10.1016/S0002-9440\(10\)61776-2](https://doi.org/10.1016/S0002-9440(10)61776-2).
- [26] X.S. Ren, Y. Tong, L. Ling, D. Chen, H.J. Sun, H. Zhou, X.H. Qi, Q. Chen, Y.H. Li, Y.M. Kang, G.Q. Zhu, NLRP3 gene deletion attenuates angiotensin II-induced phenotypic transformation of vascular smooth muscle cells and vascular remodeling, *Cell. Physiol. Biochem.* (2018), <https://doi.org/10.1159/000486061>.
- [27] E.I. Elliott, F.S. Sutterwala, Initiation and perpetuation of NLRP3 inflammatory activation and assembly, *Immunol. Rev.* 265 (2015) 35–52, <https://doi.org/10.1111/imr.12286>.
- [28] Y. He, H. Hara, G. Núñez, Mechanism and regulation of NLRP3 inflammasome activation, *Trends Biochem. Sci.* (2016), <https://doi.org/10.1016/j.tibs.2016.09.002>.
- [29] H. Okamoto, Osteopontin and cardiovascular system, *Mol. Cell. Biochem.* (2007), <https://doi.org/10.1007/s11010-006-9368-3>.
- [30] M.R. Bennett, Apoptosis in the cardiovascular system, *Heart* (2002), <https://doi.org/10.1136/heart.87.5.480>.
- [31] A. Farshid, *N. Engl. J. Med.* 375 (2016) 2604, <https://doi.org/10.1056/NEJMc1613866>. To the editor.